Biowaste sago bark based catalyst free carbon nanospheres: Waste to wealth approach

Gurumurthy Hegde,[a] Shoriya Aruni Abdul Manaf,[b] Anuj Kumar,[c] Gomaa A M Ali,[b] Kwok Feng Chong,[b] Zainab Ngaini,[d] and K V Sharma[e]*

* [a] BMS R & D Centre, BMS College of Engineering, Basavanagudi, Bangalore, 560019, India. E-mail: murthyhegde@gmail.com

[b] Faculty of Industrial Sciences and Technology, Universiti Malaysia Pahang, 26300, Gambang, Kuantan, Malaysia.

[c] Czech Technical University in Prague, Faculty of Civil Engineering, Department of Building Structures, Thákurova 7, 166 29 Praha 6 - Dejvice, Czech Republic.

[d] Department of Chemistry, Faculty of Resource Science and Technology, Universiti Malaysia Sarawak, 94300, Sarawak, Malaysia.

[e] Department of Mechanical Engineering, University Technology Petronas, Bandar Seri Iskandar,31750, Tronah, Perak, Malaysia.

Keywords: sago bark • nanoporous carbon • pyrolysis • supercapacitors • waste to wealth

ABSTRACT: Catalyst free carbon nanospheres were synthesized using simple one step pyrolysis techniques where biowaste sago bark is used as a carbon precursor. Obtained carbon nanospheres showed porous nature and revealed that more than 95% carbon is present in the synthesized carbon nanospheres with particle size ranging from 40-70 nm. Electrochemical study showed specific capacitance value of 180 Fg^{-1} at 2 mVs^{-1} and the cycling stability up to 1700 cycles. Obtained carbon nanospheres are useful in super capacitor applications. Presented study revealed waste to wealth approach thereby reducing waste in the environment.

INTRODUCTION

Carbon based nanomaterials have promising applications in nanoelectronics [1], microelectrical devices [2], electrochemistry [3,4], sensors [5], catalysis [6] and ultracapacitors [7–9]. Among different forms of carbon nanomaterials [10-13], carbon nanospheres are gaining interest because, in its spherical arrangement they are normally unclosed shells with rather waving flakes that follow the curvature of the sphere. This forms many open edges at the surface creating reactive ‘‘dangling bonds’’ which provides the spheres with high chemical activity; establishing them as good candidates for their use in various applications [11].

Various methods have been reported for the synthesis of carbon nanospheres transition and/or rare earth metal oxides as catalysts [14], carbon nanospheres from the carbonization of polyethylene–poly-(vinyl chloride) in a sealed gold tube under a pressure of 30 MPa [15], in carbon vapor from the decomposition of β-SiC powder [16] etc. Carbon nanospheres of 20–500 μm are found as a side product in the synthesis of fullerene by the deposition of gaseous carbon [17]. Arc discharge and laser ablation methods have also been used for the synthesis of structured carbon [18, 19]. Although the catalytically assisted chemical vapour deposition method is emerged as a promising technique [20], an economically viable method for the

preparation of bulk quantity of carbon nanospheres under reasonable experimental conditions is still lacking to date. Many methods use petroleum products as a source for carbon material preparation which has got negative environmental impact and also these methods suffer from many problems such as production of significant quantity of undesired by-products, additional purification steps, low yields and high energy requirements, high cost production etc. Thus, the need in alternate carbon sources for the synthesis of environmentally friendly, cost effective carbonaceous materials is the present day's requirement.

On the other hand carbon materials with high degree of porosity and high specific surface area are employed in the development of advanced energy storage systems such as electrochemical capacitors [21-25]. Electrical/electrochemical double layer capacitor (EDLC) also known as "super-capacitor" or "ultra-capacitor", is a promising one, which is characterized by energy density in the range of 1-10 Wh/kg and power density of 1-10 kW/kg. These high parameters influence the replacement of the batteries as a storage media by EDLC in many systems where traditional batteries are used (e.g. hybrid electric vehicles, power back-up systems, UPS etc.). Very recently we came up with an alternate source for the fabrication of carbonaceous material and reported the porous carbon nanoparticles and its electrochemical applications [26-28]. Apart from this, direct laser writing of micro-supercapacitors on hydrated graphite oxide films also reported as excellent materials for supercapacitors [29].

In our continued investigation, herein we report the synthesis of carbon nanospheres (CNSs) by a catalyst free pyrolysis technique from bio-waste sago bark, which is an inexpensive fibrous residue obtained from sago palm tree. The prepared CNSs are characterized using various characterization techniques to prove its spherical shape and also for its ability to use as potential materials for super capacitor application. The advantage of the presented method is that, the

described process can be applied in bulk synthesis and also it is environment friendly. It is also a bold step to use waste materials into useful product by utilizing waste to wealth concept.

RESULTS AND DISCUSSIONS

Sago bark is the waste solid residue resulted from the sago starch processing industries. Because of its cellulosic-hemicellulose and lignin content, sago bark can be used for sustainable development; bio-waste to wealth management. Thus, in the present work, sago bark is used as a raw material for the production of carbon nanospheres (CNSs) by a simple environmentally benign pyrolysis technique. This technique yielded the CNSs of highly ordered ultra-small sized nanospheres of carbon.

Sago bark was subjected to the TGA analysis to set the pyrolysis temperature (Figure S1-s1). In the TGA curve of sago bark, the carbonization peak appeared around 80-90 °C is due to the decomposition of lattice held water of sago bark. The main carbonization peak in the range 200-450 °C centered at 320 °C with maximum weight loss (i.e. 70%) can be attributed to the decomposition of cellulose and lignin contents and another carbonization peak around 900 °C is may be due to the presence of metal oxide traces. The FESEM-EDX results also accounted for the high carbon content in the sago bark (Figure 1 (a) and (b)). Figure S1-s2 shows the stability of the CNSs after pyrolyse at 500^{o}C. One can see the stability over wide temperature range showing complete carbonization.

FTIR analysis was helpful in elucidating the functional groups of the sago bark. According to Sun et al. (1999), the cellulose fraction of sago bark consisted of xylose and glucose as the major components of the isolated hemicelluloses and small amounts of other sugars together with noticeable amounts of arabinose and galactose [30]. Lignin, on the other hand influences the structural rigidity by stiffening and holding the fibers together. In the FTIR spectrum (Figure

1(c)), the characteristic absorption bands observed around 1160 cm^{-1} and 1420 cm^{-1} can be assigned to hemicelluloses and cellulose respectively. This may be ascribed to glycosidic linkage C-O-C. The strong stretching vibration band observed around 1643 cm^{-1} can be assigned to carbonyl group, (C = O) which gives an evidence for the high carbon content of sago bark [31-32]. Along with this, the other numerous absorption bands due to structural diversity of celluloses and hemicelluloses [33] which includes C-OH, C-H, -C-C-O functional groups were observed in the region 2931 and 1500-900 cm^{-1}. The bands at 1160 and 1035 cm^{-1} suggests the presence of arabinosyl residues and α-glucan of hemicelluloses [34]. The absorption peak at 575 cm^{-1} might appear due to presence of some oxide particle accumulations in sago bark. Hence the observed results are in accordance with the literature record. Thus, the fibrous residue with coarse nature may acts as the inbuilt template for the formation of the nanospheres.

The XRD spectrum of sago bark exhibited two peaks which are related to the microcrystalline nature of the cellulose [35]. The first peak at $2\theta = 17.74^{o}$ corresponding to (1 1 0) and the second at $2\theta = 22.09^{o}$ corresponding to (1 2 0) plane respectively (Figure 1(d)). Thus, as it is evident from the EDX analysis, FTIR and XRD studies also highlight for the high content of carbon in sago bark. These observations prompted us to fabricate nanoparticles at a pyrolysis temperature of 500 ^{o}C which contributed to the formation of highly ordered CNSs. Although these temperatures are not optimum but good enough to show the potentiality of the materials. More study is in progress to check the higher temperature effects in these direction.

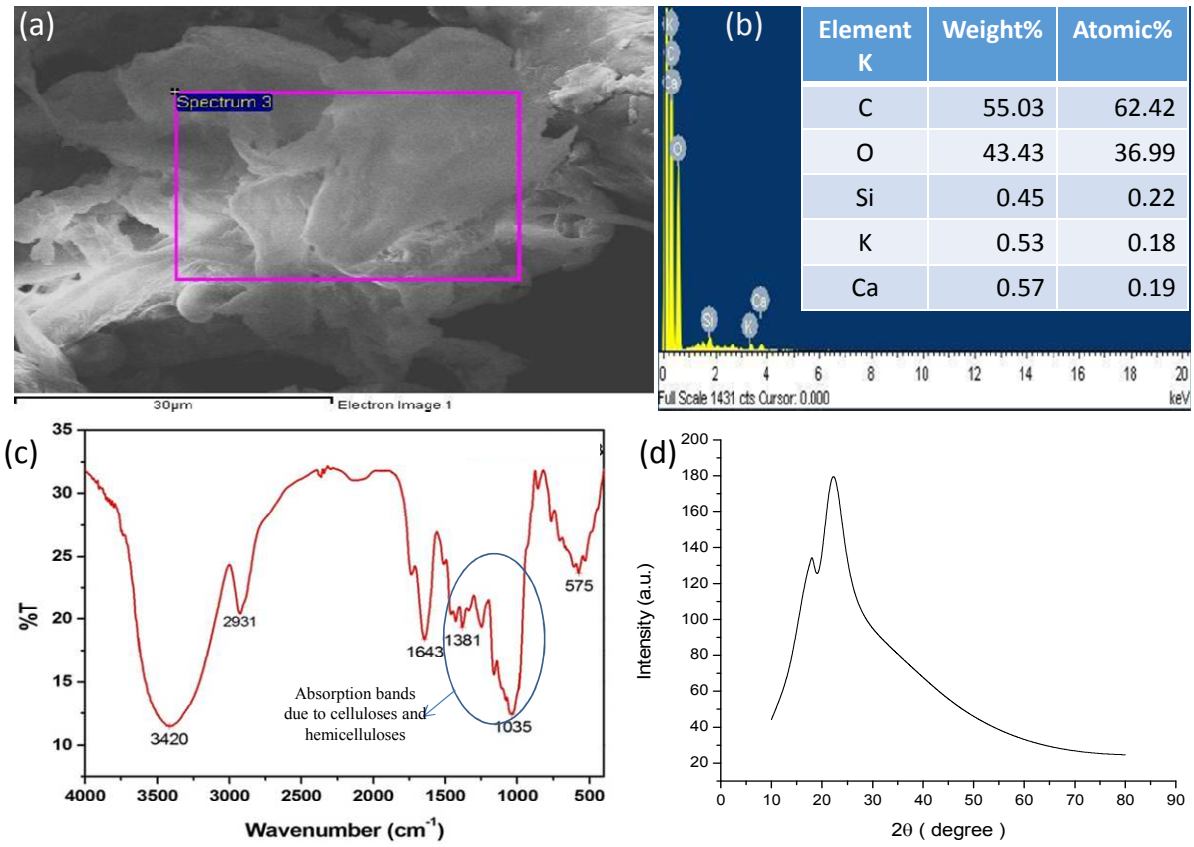

Figure 1. (a) FESEM image of raw sago bark, and (b) EDX spectrum taken from square area in Figure (a), (c) FT-IR spectrum, and (d) wide-angle XRD pattern of raw sago bark.

The raw sago bark particles were pyrolyzed in tube furnace at 500 ^{o}C for 2 hours under the continuous flow of N_2. Finally, the pyrolized products were washed with HCl solution and then with deionized water. TEM revealed the formation of uniformly distributed sphere shaped carbon nanoparticles at 500 ^{o}C pyrolysis temperature (Figure 2 (a) (b)). One can see the high porous nature of the CNSs when it is zoomed (Figure 2 (b)). The average particle size is 65 ± 5 nm as obtained from histogram (Figure 2(c)). The FESEM images (Figure 2 (d) (e)) also exhibited similar shape for the carbon nanoparticles, also the magnified image of CNSs confirm this porous structure formation (Figure 2 (e)). The wide distributions of the nanoparticles (~50

nm) were observed in histogram of the FESEM images (Figure 2 (f)). The energy dispersive X-ray (EDX) analysis showed very high percentage content of carbon using biowaste materials (~95% atomic percentage) in the prepared nanospheres (Figure S1-s3). The TEM and FESEM results suggest the conversion of bio-waste raw sago bark into carbon nanoparticles with uniform particle size possessing high carbon content belonging to the class of carbon nanospheres (CNSs) by a facile catalyst free pyrolysis technique. This was further ascertained by FTIR analysis of CNSs (Figure S1-s4). A large deviation in the bands of lignocelluloses in the region 1500-900 cm^{-1} was observed in CNSs FTIR spectrum. This may be due to the conversion of fibrous residue of sago bark into carbon nanospheres. The strong absorption band around 1635 cm^{-1} were assigned to (C=O) bond of carbonyl group. The absorption bands around 3457 and 2900 cm^{-1} are assigned to the C-OH and C-H stretching modes of the carbon skeleton.

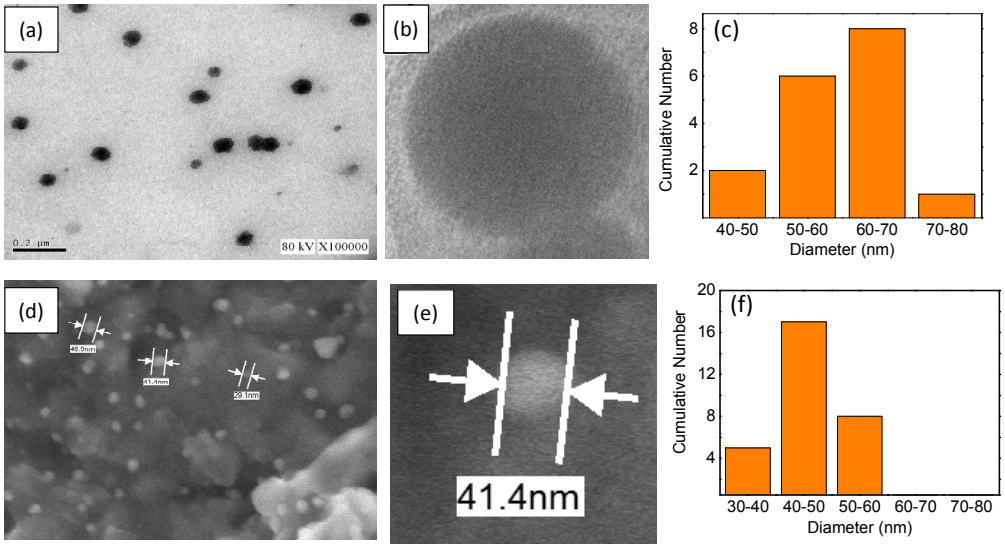

Figure 2. (a) (b) TEM image, (c) the particle size distribution histogram for CNSs for TEM (d)(e) FESEM image for CNSs. and (f) the particle size distribution histogram for CNSs for FESEM. The curve in figure (c) and (f) shows the average particle size.

The porous nature was investigated by the Brunauer-Emmett-Teller (BET) method. In IUPAC classification, the pore with diameters less than 2 nm are classified as micropore, whereas the pore with diameters from 2 to 50 nm are classified as mesopore. For the CNSs treated at 500 °C, the BET surface area (S_{BET}) is 58 $m^2 \cdot g^{-1}$ and t-plot micropore surface area (St-plot) is 32 $m^2 \cdot g^{-1}$. The $S_{t\text{-}plot}/S_{BET}$ value is quite high (55.2%), meaning large contribution from the micropores. Hence, the fabricated CNSs exhibited good microporous structure. Fig. 3 shows the nitrogen soprtion curve and pore distribution of CNSs.

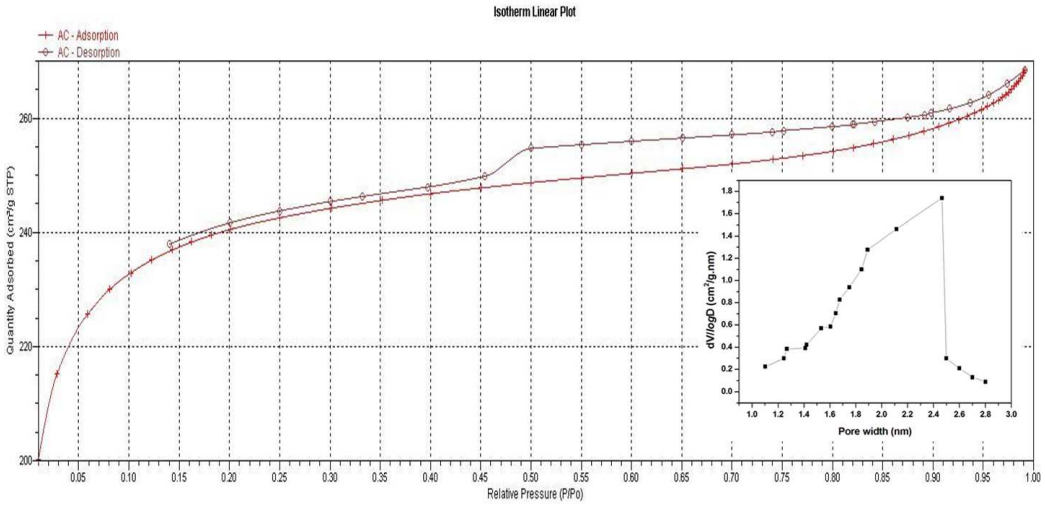

Figure 3: Adsorption and desorption curve of liquid nitrogen during BET analysis of CNSs and . BJH pore distribution in prepared CNSs.

X-ray analysis showed that, the CNSs possess crystalline and graphitic characteristic with prominent (0 0 2) and (1 0 1) plane. The CNSs exhibited a main diffraction peak at $2\theta = 26.96^o$ corresponding to (0 0 2) plane which can be attributed to graphite-2H (ICDD 411487) as shown in Figure 4(a). Quantitative measurement of graphitic character, the interlayer d- spacing d_{002} is 3.5005 Å [36]. The XRD spectrum showed a peak at $2\theta = 43.98^o$ with interlayer d-spacing 2.064

Å, which can be assigned to (1 0 1) lattice planes of graphite [37]. Very surprisingly CNSs exhibited very small peak (almost negligible) peak at 2θ = 21.0339^{o} with d_{002} = 4.2201 Å. This peak may be arisen from the highly crystalline cellulose fibres i.e., hemicelluloses and celluloses of sago bark [35, 38, 39]. Thus, the XRD analysis suggests the evolution of new class of carbon nanomaterial with high graphitic nature of the CNSs.

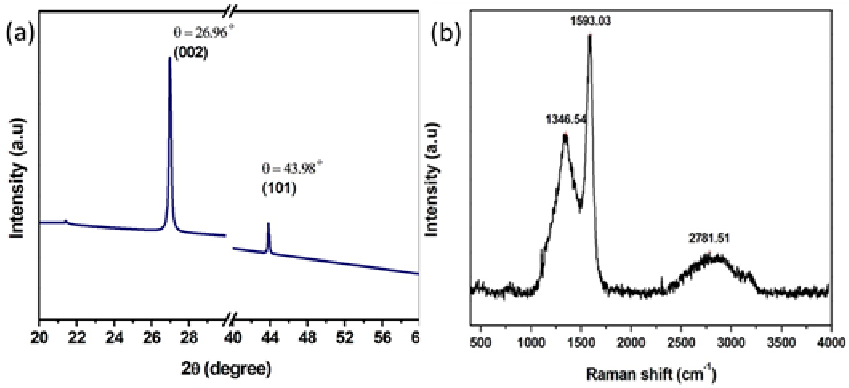

Figure 4. (a) Wide angle XRD pattern and (b) Raman spectrum of CNSs.

Raman spectroscopy is extremely useful in deducing the graphitic characteristic of carbon nanomaterial. The carbon materials present two main peaks; diagnostic of disorder in the carbon structure denoted as D- and the diagnostic of structural order denoted as G- bands. In the present CNSs, obtained at pyrolysis temperature 500 ^{o}C (Figure 4(b)), the D- band was observed at 1346 cm^{-1}. The CNSs exhibited G- band at 1593 cm^{-1} which is related to the sp^{2} bonded carbon atom from stretching modes of C = C bonds corresponding to the E_{2g} mode of graphite [40, 41]. The graphitic character can further be assessed by the relative intensities of D- and G- bands (I_D/I_G) and full-width at half-maximum (FWHM) of the G- band. In present case I_D/I_G ratio was found to be 0.84 [42] and FWHM of the G- band is found to be 62 cm^{-1}. Apart from this we observed two peaks at 2781 and 3152 cm^{-1} which can be assigned to the second order D (2 x D) and G (2 x

G) modes respectively [43] and they are very weak compared to the D- and G- bands. Thus, Raman results together with XRD analysis gives evidence for the strong graphitic character of the prepared CNSs.

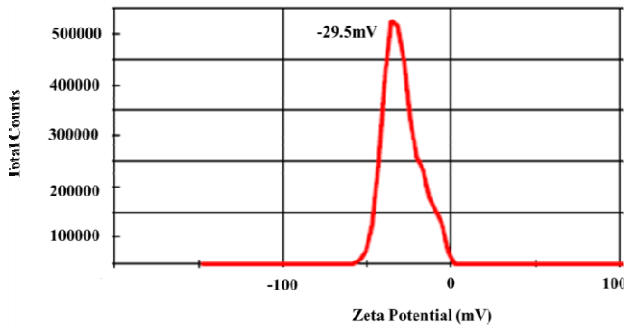

Figure 5. Zeta potential curve for aqueous solution of CNSs treated at 500 ^{o}C.

The zeta-potential is often used as an index of the magnitude of electrostatic interaction between colloidal particles and is thus a measure of the colloidal stability of the solution. The measured distributions are generally broad and asymmetric due to the range of nano-sizes and the distributions can clearly be a non-ionic. We estimated the zeta potential of the CNSs to be the centre of the distribution with zeta potential 0 mV to – 40 mV with the peak value –29.5 mV as shown in Figure 5 (phase plot is given in Figure S1-s5). So, the prepared carbon nanoparticles are stable from electrostatic considerations [44].

Due to the ever-growing populations, it is required to find the new solution for the energy demands. Supercapacitors are the ideal candidates for fulfilling energy demands to some extent. Carbon nanoparticles played vital role to handle these responsibilities. With respect to that, electrochemical properties of CNSs are presented in Figure 6 and 7. CNSs show capacitive behaviour as corroborated by CV curves measured at different scan rates which exhibit almost rectangular-like shape as shown in Figure 6 (a). The specific capacitance (Cs) values were

calculated by integrating the area under the curve. The present CNSs show Cs of 180 F g^{-1} at 2 mVs^{-1} and it is observed that the values decrease with increasing scan rate (Figure 6(b)).

Figure 5(c) presents the charge-discharge tests at different current densities. The plot indicates rapid current-voltage response. Moreover, CNSs show high Cs value of 113 F/g at 20 mAg^{-1} and decrease with increasing discharge current (Figure 6(d)). The cycling stability of CNSs was studied using galvanostatic charge–discharge at 0.2 Ag^{-1} for 1700 cycles as presented in Figure 7(a). The results show that, the cycling stability is still maintained more than 94% of its original capacitance even after 1700 cycles, indicating excellent cyclic stability. CNSs also showed high columbic efficiency of 95% as shown in Figure 7 (a). Such high capacitance retention of up to 1700 cycles suggests that the CNSs are a good candidate for supercapacitor applications.

The electrochemical impedance spectroscopy (EIS) study was carried to further investigate the electrochemical properties for CNSs. Nyquist plot for CNSs is shown in Figure 7(b). The inset of Figure 7(b) represents the high frequency region of the recorded full impedance plot. A small semicircle in the high frequency region and a vertically straight line in the low frequency region can be seen. The solution resistance (R_s) was found to be very small (0.78 Ω), indicating high electrical conductivity of CNSs. The charge transfer resistance (R_{ct}) associated with the surface electrode properties was found to be 0.26 Ω. Detail investigation in this direction is in progress to enhance the specific capacitance value by activating the carbon nanospheres and will be reported elsewhere. The Ragone plot for sago bark based carbon nanospheres is shown in Figure 7 (c), presenting the maximum energy density of 5 $Whkg^{-1}$ and maximum power density of 400 Wkg^{-1}. The energy and power densities were calculated using the equation reported elsewhere [45]. The energy density was found to be reasonable in comparison with those obtained for activated carbon [46]. The obtained high values of supercapacitance may be due to the porous

nature of carbon and high surface area. We are now in process of activating the carbon thereby increasing surface area so that one can get much superior super capacitors will be published elsewhere.

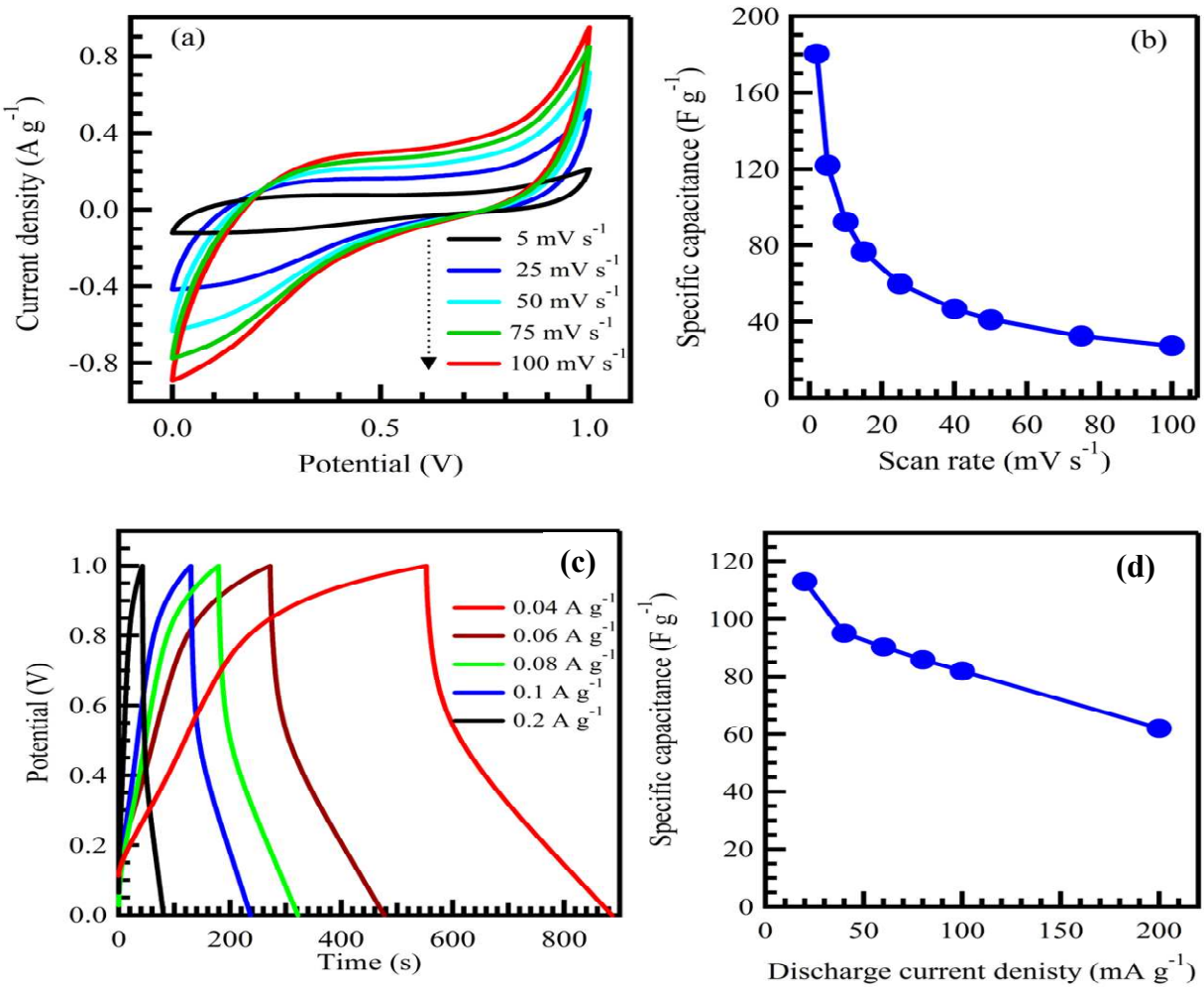

Figure 6. Electrochemical properties of CNSs: Cyclic voltammetry curves (a) at different scan rates and specific capacitance (b) as a function of scan rate. Galvanostatic charge-discharge curves (c) at different current densities and specific capacitance (d) as a function of current density.

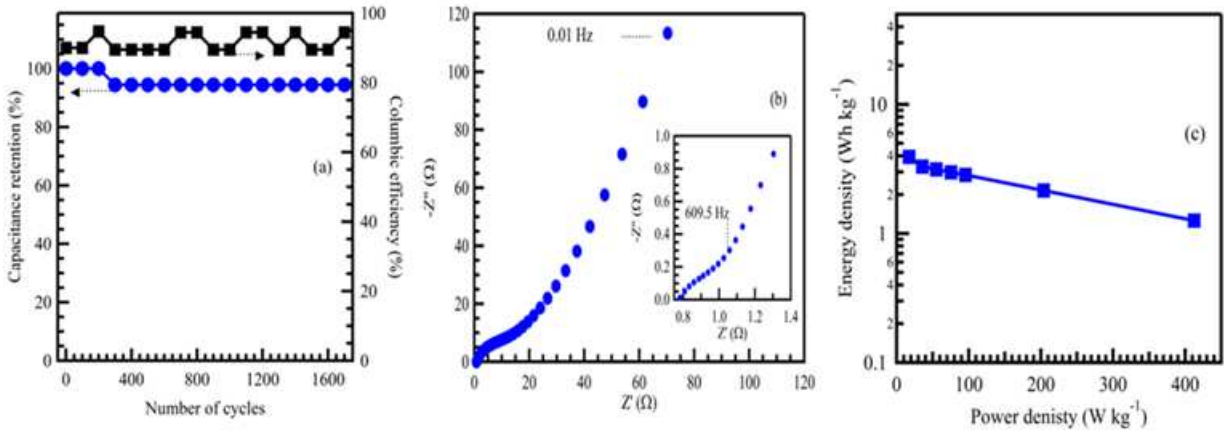

Figure 7. Electrochemical properties of CNSs showing (a) Cycle life stability curve (left vs. bottom) and coulumbic efficiency (right vs. bottom) at 0.2 Ag^{-1} current density, (b) Nyquist plots; the inset is zoomed view of Nyquist plots at high-frequency region, (c) Ragone plot.

CONCLUSION

In conclusion, simple, cost effective carbon nanospheres obtained from waste sago bark without addition of any catalyst were synthesized. Obtained CNSs show high quality particles with uniform sizes ranging from 40-70 nm along with ability to bulk produce. Due to their porous nature, they do show reasonable specific capacitance for the application of super capacitors. This is a bold step to convert biowaste materials into useful products thereby reducing pollution in the environment.

Experimental Section

Synthesis and purification of CNSs

The dry sago bark was obtained from sago palm estate in Malaysia where major sago related products were taking place and also heavy amount of waste produced from sago bark. The fibrous residue was separated and dried in an oven at 110^{o}C for two days to remove all the moisture. The dry sago bark was crushed, followed by grinding at 12000rpm using grinder (Retsch, ZM 200, Germany) and further the grind raw sago bark was sieved to the particle size

~60-70 μm. Then the raw sago bark was pyrolyzed in tube furnace (Nabertherm, EW-33334-36) at 500 ^{o}C for 2h under the continuous flow of nitrogen (N_2) (150 mlcm^{-3}) at a heating rate of 5 ^{o}C m^{-1} and simultaneously cool down to room temperature in the N_2 atmosphere to get pyrolyzed product. The pyrolized products were washed with 1M hydrochloric acid (HCl) and then with deionized water to get pure CNSs.

Characterization of CNSs

The raw sago bark and CNSs were characterized using FTIR (Perkin, Elmer Spectrum 100), FESEM-EDX (JEOL, JSM-7800F), XRD (Rigaku Mineflex II) TEM (JEOL, JSM 1230) and Themogravimetric Analysis (TGA) (METTLER TOLEDOTGA/DSC HT /1600). The BET surface area and pore width of CNSs were evaluated using Micromeritics ASAP 2020 under low pressure dose, the CNSs samples was degased for 12 h at 200 °C. The Raman spectra of CNSs were taken using HORIBA Scientific Raman spectroscopy. Zeta potential values were measured using Zetasizer Nano ZS90 obtained from Malvern Mastersizer.

Electrochemical studies

The electrodes were made by mixing CNSs with 5 wt.% polytetrafluoroethylene (PTFE) and 15 wt.% carbon black. The electrochemical tests were performed using a two-electrode type system, in which the two electrodes were electrically isolated from each other by porous membrane in 5 M potassium hydroxide (KOH) electrolyte. The data were collected using an electrochemical workstation (Autolab/PGSTAT M101) equipped with a frequency response analyzer. Cyclic voltammetry tests were performed between 0 to 1 V with scan rates range from 2 to 100 mVs^{-1}. Charge-discharge galvanostatic tests were performed at current densities up to 1 Ag^{-1}. Impedance data were collected from500 kHz to 0.01 Hz, with 10 mV in ac amplitude signal at open circuit potential (OCP).

AUTHOR INFORMATION

Corresponding Author

* BMS R & D Centre, BMS College of Engineering, Basavanagudi, Bangalore, 560019, India.

E-mail: murthyhegde@gmail.com , hegde@bmsce.ac.in

Author Contributions

[a*] Hegde Gurumurthy contributed in designing, analyzing and writing the manuscript

[b] Shoriya Aruni contributed in conducting experiments and also analyzing the experiments.

[c] Gomaa A.M. Ali and Kwok Feng Chong contributed in electrochemical studies of CNSs.

[c] Kumar Anuj contributed in characterizing and also writing the manuscript.

[d] Zainab Ngaini is responsible for measuring and characterization of TEM of the CNSs.

[e]K V Sharma is responsible for measuring and characterization of the Raman spectra of the CNSs.

ABBREVIATIONS

FESEM : Filed Emission Scanning Electron Microscopy, TEM: Transmission Electron Microscopy, XRD: X-ray Diffraction, PCN: Porous Carbon Nanospheres, BET: Brunauer-Emmett-Teller, FTIR: Fourier Transform Infrared, TGA:Thermo Gravimetric Analysis.

ACKNOWLEDGEMENTS

One of the author AK would like to acknowledge the European social fund within the framework of realizing the project “Support of inter-sectoral mobility and quality enhancement of research teams at Czech Technical University in Prague”, CZ.1.07/2.3.00/30.0034.

SUPPORTING INFORMATION

This material is available free of charge via the Internet at http://pubs.acs.org

REFERENCES

1. C. Berger, Z. Song, X. Li, X. Wu, N. Brown, C. Naud, D. Mayou, T. Li, J. Hass, AN. Marchenkov, EH. Conrad, PN. First, de Heer. WA. Electronic confinement and coherence in patterned epitaxial graphene. *Science*. **2006**, *312*, 1191.

2. S. Gilje, S. Han, M. Wang, KL. Wang, RB. Kaner. A chemical route to graphene for device applications. *Nano Lett*. **2007**, *7(11)*, 3394-3398.

3. YG. Guo, YS. Hu, J. Maier. Synthesis of hierarchically mesoporous anatase spheres and their application in lithium batteries. *Chem Commun*. **2006**, 2783–2785.

4. ZY. Yuan, BL. Su. Insights into hierarchically meso-macroporous structured materials. *J Mater Chem*. **2006**, *16(7)*, 663–677.

5. L. Quercia, F. Loffredo, B. Alfano, V. La Ferrara, G. Di Francia. Fabrication and characterization of carbon nanoparticles for polymer based vapour sensors. *Sens Actuators B: Chem*. **2004**, *100(1)*, 22–28.

6. Y. Li, X. Fan, J. Qi, J. Ji, S. Wang, G. Zhang, F. Zhang. Palladium nanoparticle-graphene hybrids as active catalysts for the Suzuki reaction. *Nano Res*. **2010**, *3(6)*, 429–437.

7. J. Lee, S. Yoon, T. Hyeon, S. Oh, K. Kim. Synthesis of a new mesoporous carbon and its application to electrochemical double-layer capacitors. *Chem Commun*. **1999**, *21,* 2177–2178.

8. H. Yang, Q. Shi, X. Liu, S. Xie, D. Jiang, F. Zhang, C. Yu, B. Tu, D. Zhao. Synthesis of ordered mesoporous carbon monoliths with bicontinuous cubic pore structure of Ia 3 d symmetry. *Chem Commun*. **2002**, *23,* 2842–2843.

9. MD. Stoller, S. Park, Y. Zhu, J. An, RS. Ruoff. Graphene-based ultracapacitors. *Nano Lett*. **2008**, *8(10)*, 3498–3502.

10. M. Thunga, K. Chen, D. Grewell, M.R. Kessler. Bio-renewable precursor fibers from lignin/polylactide blends for conversion to carbon fibers. *Carbon*. **2014**, *68*, 159–166.

11. M. Golshadi, J. Maita, D. Lanza, M. Zeiger, V. Presser, M.G. Schrlau. Effects of synthesis parameters on carbon nanotubes manufactured by template-based chemical vapor deposition. *Carbon*, **2014,** *80*, 28-39.

12. H. Pan, J. Zang, X. Li, Y. Wang. One-pot synthesis of shell/core structural N-doped carbide-derived carbon/SiC particles as electrocatalysts for oxygen reduction reaction. *Carbon*. **2014**, *69*, 630–633.

13. J. Y. Miao, D. W. Hwang, K. V Narasimhulu, P. I. Lin, Y. T. Chen, S. H. Lin, L. P Hwang. Synthesis and properties of carbon nanospheres grown by CVD using Kaolin supported transition metal catalysts. *Carbon*, **2004**, *42*(4), 813-822.

14. ZL. Wang, ZC. Kang. Pairing of pentagonal and heptagonal carbon rings in the growth of nanosize carbon spheres synthesized by a mixed-valent oxide-catalytic carbonization process. *J Phys Chem B*. **1996**, *100(45)*, 17725-17731.

15. M. Inagaki, K. Kuroda, M. Sakai. Pressure carbonization of polyethylene-polyvinylchloride mixtures. *Carbon*. **1983**, *21(3)*, 231-235.

16. K. Yamada, S. Tobisawa. Structure and formation process of carbon blacks formed by decomposing SiC powder using a conically converging shock-wave technique. *Carbon*. **1989**, *27(6)*, 845-852.

17. I. Loa, C. Moschel, A. Reich, W. Assenmacher, K. Syassen, M. Jansen. Novel graphitic spheres: Raman spectroscopy at high pressures *Phys Stat Sol (b)*. **2001**, *223(1)*, 293-298.

18. M. Glerup, J. Steinmetz, D. Samaille, O. Stephan, S. Enouz, A. Loiseau, S. Roth, P. Bernier. Synthesis of N-doped SWNT using the arc-discharge procedure. *Chem Phys Lett*. **2004**, *387(1)*, 193–197.

19. Y. Zhang, H. Gu, K. Suenaga, S. Iijima. Heterogeneous growth of B□ C□ N nanotubes by laser ablation *Chem Phys Lett*. **1997**, *279(5)*, 264–269.

20. K.P. De Jong, JW. Geus. Carbon nanofibers: catalytic synthesis and applications. *Catal Rev Sci Eng*. **2000**, *42(4)*, 481–510.

21. V. Subramanian, C. Luo, AM. Stephan, KS. Nahm, S. Thomas, B. Wei. Supercapacitors from activated carbon derived from banana fibers *J Phys Chem.* **2007**, *111(20)*, 7527-7531.

22. M. Endo, Y. Kim, K. Osawa, K. Ishii, T. Inoue, T. Nomura, N. Miyashita, MS. Dresselhaus. High Capacitance EDLC Using a Carbon Material Obtained by Carbonization of PVDC The

Effect of the Crystallite Size of the Pristine PVDC.*Electrochem Solid State Lett*. **2003**, *6(2)*, A23-A26.

23. G. Lv, D. Wu, R. Fu, Z. Zhang, Z. Su. Electrochemical properties of conductive filler/carbon aerogel composites as electrodes of supercapacitors. *J Non-Cryst Solids*. **2008**, *354(40)*, 4567-4571.

24. E. Frackowiak, K. Metenier, V. Bertagna, F. Beguin. Supercapacitor electrodes from multiwalled carbon nanotubes. *Appl Phys Lett*. **2000**, *77(15)*, 2421-23.

25. An, K. H., Kim, W. S., Park, Y. S., Choi, Y. C., Lee, S. M., Chung, D. C., ... & Lee, Y. H. Supercapacitors using single-walled carbon nanotube electrodes. *Advanced Materials*, **2001**, *13*(7), 497-500.

26. Anuj Kumar, Gurumurthy Hegde, S. A. B. Abdul Manaf, Z. Ngaini and K. V. Sharma, Catalyst free silica templated porous carbon nanoparticles from bio-waste materials. *Chem. Comm*. **2014**, *50(84)*, 12702-12705.

27. G. A. M. Ali, S. A. B. Abdul Manaf, Anuj Kumar, K. F. Chong and Gurumurthy Hegde, High performance supercapacitor using catalysis free porous carbon nanoparticles. *J. Phy. D: App. Phy*. **2014**, *47*, 495307-495312.

28. S. A. B. Abdul Manaf, Partha Roy, Korada V.Sharma, Zainab Ngaini, V.Malgras, A.Aldalbahi, S.M.Alshehri, Y.Yamauchi, Gurumurthy Hegde, Catalyst-free synthesis of carbon nanospheres for potential biomedical applications: waste to wealth approach. *RSC Adv*. **2015**, *5*, 24528-24533.

29. W.Gao, N.Singh, Li. Song, Z. Liu, A.L.M. Reddy, L. Ci, R. Vajtai, Q. Zhang, B. Wei, P. M. Ajayan. Direct laser writing of micro-supercapacitors on hydrated graphite oxide films. *Nature*. 2011, **6**, 496-500.

30. RC. Sun, GL. Jones, J. Tomkinson ,J. Bolton. Fractional isolation and partial characterization of non-starch polysaccharides and lignin from sago pith. *Ind. Crops Prod*. **1999**, *9(3)*, 211-220.

31. SF. Sim, M. Mohamed, N.A.L.M.I. Lu, N.S.P. Sarman, S.N.S. Samsudin. Computer-assisted analysis of Fourier Transform Infrared (FTIR) spectra for characterization of various treated and untreated agriculture biomass. *BioResources*. **2012**, *7(4)*, 5367-5380.

32. CH. Cheng, J. Lehmann, J.E. Thies, SD. Burton, MH. Engelhard Oxidation of black carbon by biotic and abiotic processes. . *Org Geochem*. **2006**, *37(11)*, 1477-1488.

33. F. Peng, JL. Ren, F. Xu, J. Bian, P. Peng, RC. Sun. Comparative study of hemicelluloses obtained by graded ethanol precipitation from sugarcane bagasse. *J Agric Food Chem*. **2009**, *57(14)*, 6305-6317.

34. M. Kacurakova, P. Capek, V. Sasinkova, N. Wellner, A. Ebringerova. FT-IR study of plant cell wall model compounds: pectic polysaccharides and hemicelluloses. *Carbohyd Polym*. **2000**, *43(2)*, 195-203.

35. A. P. Mathew, K. Oksman and M. Sain, Mechanical properties of biodegradable composites from poly lactic acid (PLA) and microcrystalline cellulose (MCC). *J. App. Poly. Sci*. **2005**, *97(5)*, 2014-2025.

36. Z. Li, D. Wu, Y. Liang, F. Xu , R. Fu. Facile fabrication of novel highly microporous carbons with superior size-selective adsorption and supercapacitance properties. *Nanoscale*. **2013**, *5(22)*, 10824-10828.

37. S. Kuga, D.-Y. Kim, Y. Nishiyama and R. M. Brown. Nanofibrillar carbon from native cellulose. *Mol. Cryst. Liq. Cryst*. **2002**, *387(1)*, 13–19.

38. Z.-Y. Wu, C. Li, H.-W. Liang, J.-F. Chen and S.-H. Yu. Ultralight, Flexible, and Fire-Resistant Carbon Nanofiber Aerogels from Bacterial Cellulose. *Angew. Chem., Int. Ed.* **2013**, *52(10)*, 2925–2929.

39. D. Klemm, B. Heublein, H.-P. Fink and A. Bohn. Cellulose: fascinating biopolymer and sustainable raw material. *Angew. Chem., Int. Ed.* **2005**, *44(22)*, 3358–3393.

40. Y. Li, J. Chen, Q. Xu, L. He, Z. Chen. Controllable route to solid and hollow monodisperse carbon nanospheres. *J. Phys. Chem. C*. **2009**, *113(23)*, 10085–10089.

41. Y. Li, E. J. Lee, W. P. Cai, K. Y. Kim and S. O. Cho. Unconventional method for morphology-controlled carbonaceous nanoarrays based on electron irradiation of a polystyrene colloidal monolayer. *ACS Nano*. **2008**, *2(6)*, 1108-1112.

42. H.S. Qian, F. M. Han, B. Zhang, Y.C. Guo, J. Yue, B.X. Peng. Non-catalytic CVD preparation of carbon spheres with a specific size *Carbon.* **2004**, *42(4)*, 761–766.

43. J.Y. Miao, D. W. Hwang, K.V. Narasimhulu, P.I. Lin, Y.T. Chen, S.H. Lin, L.P. Hwang. Synthesis and properties of carbon nanospheres grown by CVD using Kaolin supported transition metal catalysts. *Carbon.* **2004**, *42(4)*, 813–822.

44. B. White, S. Banerjee, S. O'Brien, N.J. Turro, P.I. Herman. Zeta-potential measurements of surfactant-wrapped individual single-walled carbon nanotubes. *J. Phys. Chem. C*. **2007**, *111(37)*, 13684-13690.

45. C. Liu, Z. Yu, D. Neff, A. Zhamu, BZ. Jang. Graphene-based supercapacitor with an ultrahigh energy density. *Nano Lett*. **2010**, *10(12)*, 4863-4868.

46. P.Kleszyk, , P. Ratajczak, P. Skowron, J. Jagiello, Q. Abbas, E. Frackowiak, and F. Béguin. Carbons with narrow pore size distribution prepared by simultaneous carbonization and self-activation of tobacco stems and their application to supercapacitors. *Carbon,* **2015***, 81,* 148-157.

For Table of Contents Only

Biowaste sago bark based catalyst free carbon nanospheres: Waste to wealth approach

Gurumurthy Hegde, [a] Shoriya Aruni Abdul Manaf,[b] Anuj Kumar,[c] Gomaa A M Ali,[b] Kwok Feng Chong,[b] Zainab Ngaini,[d] and K V Sharma[e]*

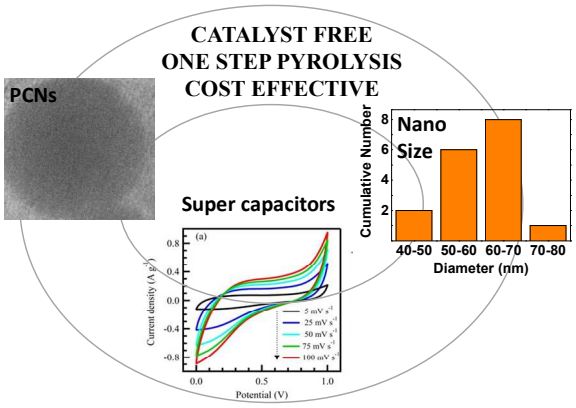

Template free, catalyst free, cost effective carbon nanospheres obtained using biowaste sago bark with simple cost effective pyrolysis techniques gives high content of carbon which can be used for super capacitor applications. Waste to wealth approach is adapted in which one can use waste materials into useful products.